JOURNAL OF SPACECRAFT AND ROCKETS
Vol. 36, No. 4, July–August 1999

Payload Fairing Separation Dynamics

S.-C. Cheng*
The Aerospace Corporation, Los Angeles, California 90009-2957

Launch vehicle fairings protect payloads from aerodynamic loads during atmospheric flight. Once the launch vehicle is outside the atmosphere, the fairing is jettisoned. For Titan and Delta launch systems, payload fairing separation is accomplished by detonation of an explosive charge in the separation joints. The resulting high-pressure gases force the fairing segments apart at the separation joints and thrust the sectors away from the launch vehicle. To predict the gas pressure accurately, one needs to formulate the thermodynamic processes of the charge in the separation joint at ignition, the subsequent gas flow, the nonlinear shearing of the rivets that hold the fairing segments together, and the dynamic interaction between the gas and the flexible fairing structure. An analytical procedure based on a coupled gas/structure model has been developed to simulate the fairing separation events. The procedure was validated by comparing the analysis results with full-scale payload fairing separation test data obtained by the Titan IV launch vehicle program.

Nomenclature

A	= area, m^2
C	= constant-volume specific heat, J/kg-K
D	= diameter, m
$\{F(t)\}$	= vector of system external forces, N
$\{g\}$	= vector of system generalized translations and rotations, m and rad
$\{\ddot{g}\}$	= vector of system generalized accelerations, m/s^2 and rad/s^2
Hg	= latent heat of gasification, J/kg
$[K]$	= physical system stiffness matrix, N/M and N/rad
M, m	= mass of gases, kg
$[M]$	= physical system mass matrix, kg
$[m]$	= mass submatrix, kg
p	= pressure, N/m^2 or bar
p_r	= pressure ratio, dimensionless
Q	= heat gained or lost, J
$\{Q\}$	= vector of regeneralized translations and rotations, m and rad
$\{\dot{Q}\}$	= vector of regeneralized velocities, m/s and rad/s
$\{\ddot{Q}\}$	= vector of regeneralized accelerations, m/s^2 and rad/s^2
R	= gas constant, J/kg-K
T	= temperature, K
Ta	= ambient temperature, K
U	= internal energy of gases, J
$\{u(t)\}$	= vector of physical system translations and rotations, m and rad
$\{\ddot{u}(t)\}$	= vector of physical system accelerations, m/s^2 and rad/s^2
v	= cell volume, m^3
v_r	= volume ratio, dimensionless
$\dot{w}$	= mass flow rate, kg/s
γ	= specific heat ratio, dimensionless
$[\xi]$	= modal damping ratio matrix, dimensionless
ρ	= density, kg/m^3
$[\Phi]$	= regeneralized system modes matrix, dimensionless
$[\phi]$	= system modes matrix, dimensionless
$[\omega]$, $[\Omega]$	= matrix of circular frequencies, rad/s

Subscripts

a	= attachment or ambient
d	= downstream
in, out	= direction of flow
n	= normal or incremental counter
p	= bellows
r	= rivets
u	= upstream
1	= PETN gas
2	= gasified polyester
12	= mixed gas

Received 2 December 1995; revision received 23 October 1998; accepted for publication 2 November 1998.

This paper is dedicated to the memory of S.-C. Cheng.

*Engineering Specialist, Structural Dynamics Department, P.O. Box 92957-M4/909 (Deceased).

Introduction

As shown in Fig. 1, the Titan IV payload fairing (PLF) is separated into three segments after the vehicle leaves the atmosphere. The separation is accomplished by detonation of a linear explosive charge, which expands the flexible bellows with pressurized gases, forcing the shearing of the rivets and pushing the trisector segments of the fairing away from the vehicle. The rivet pattern along the separation joint is designed to provide adequate resistance to flight air loads. Design of the PLF separation system requires that adequate energy be available to shear all of the rivets and jettison the three fairing segments, providing sufficient separation velocity to prevent recontact with the advancing payload/booster, while keeping the shock level within the capability of the sensitive equipment on board the payload and booster.

It is important to establish the remaining energy left in the separation system after the energy needed for shearing the rivets is spent. To ensure that enough remaining energy, or force margin, is in the PLF separation system, two test configurations are used in the full-scale separation test: the flight configuration and a force-margin configuration. As shown in Fig. 1, the inner tube contains three strands of charge in the linear explosive assembly (LEA) for a flight configuration. For the force-margin test configuration, only two strands are placed in the LEA. The flight configuration test is to measure the performance of the flight PLF design. The successful separation of the PLF in a force-margin test ensures that at least a 50% force margin exists, a level considered sufficient for this type of system. High-speed cameras and pressure transducers are used to measure the separation velocities and bellows pressure transients in both the flight and the force-margin separation tests. In January 1988, a full-scale fairing separation test was conducted at Arnold Engineering Development Center (AEDC) for a specific Titan IV PLF flight configuration (three-strand LEA and flight rivet pattern). In March 1988, a second test was performed for the force-margin configuration (two-strand LEA). The work presented in this paper is part of the effort to predict the test results analytically and to correlate with the test data.[1]

Full-scale tests are very expensive to conduct because the tests need to be performed in a vacuum chamber to simulate proper altitude conditions. With a fleet of Titan IV PLFs of different lengths, it was impractical to test all of them. Therefore, it was highly desirable

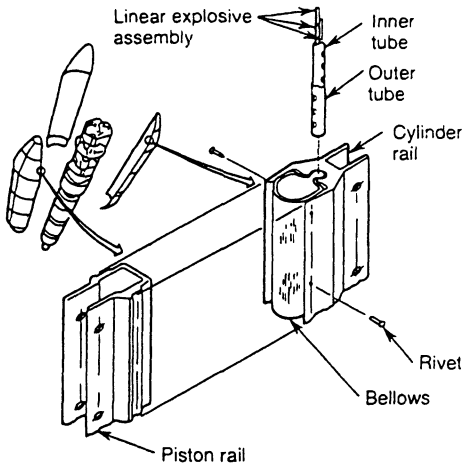

Fig. 1 PLF separation joint.

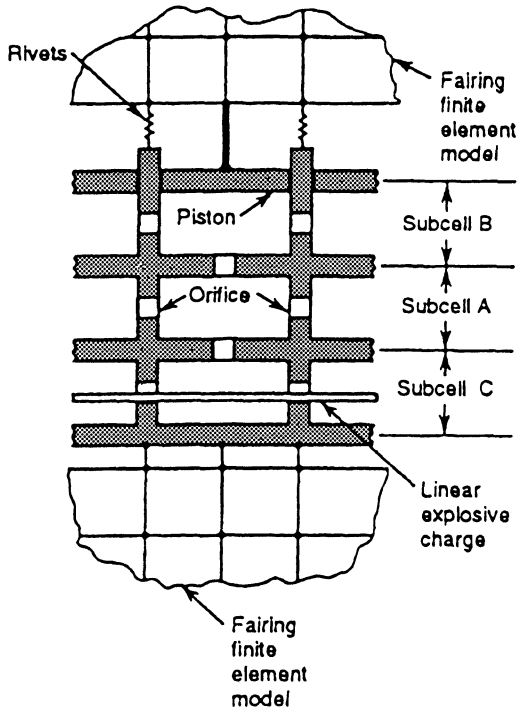

Fig. 2 Coupled gas/structure model.

to provide an analytical tool to simulate the PLF separation event and use the existing test results to verify the analytical procedure. The development of this analytical procedure is described. First, the coupled structure/gasdynamic model for the fairing separation simulation is presented. The detailed formulation of the thermodynamic process during the ignition of the charge and the subsequent gas flow in the actuator tubes and bellows is presented next. This is followed by the description of the structural model, the governing equations of motion for the coupled system, and the numerical solution procedure. A comparison between the analytical results and the test data is also presented from which some conclusions are drawn.

PLF Separation Model

The PLF separation system (Fig. 1) consists of two interlocking rails with a folded bellows between them. The two rails are held together by rivets. Inner and outer tubes are placed inside the bellows, with linear explosive charge strands inside the inner tube. Both tubes have venting holes to allow the ignition gas to flow into the bellows. To simulate this system, a coupled gas/structure model was devised, as shown in Fig. 2. The two rails are represented as a piston and cylinder system. The gas model consists of a series of interconnecting cells along the length of the separation joint. Each cell is further divided into three subcells representing specific control volumes of the attenuation/bellows assembly. The subcells are connected to each other by orifices to form a gas flow network. It should be noted that the volume of subcell C, which represents the interior of the bellows, is controlled by the displacement of the piston, which is slaved to the fairing finite element model. The deformation of the finite element model will affect the volume and, thus, the pressure inside the bellows. The coupling between the gas system and structural dynamic response is mainly due to this interaction between the gas and structural models.

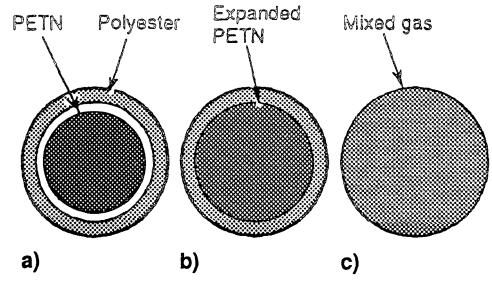

Fig. 3 Gas expansion in a single strand.

The detonation of the charge is initiated by detonators, which are usually located at the top and bottom of the fairing. A typical gas cell located at a distance, for example, x_i, from the nearest detonator will start to burn at time $t_i = x_i/V$, where V is the burning propagation speed along the strand. The thermodynamic process in this typical cell starts at time t_i, as described in the next section.

Gas Expansion in Inner Tube

In this section, the high-temperature gas expansion in the inner tube is described. It is assumed that this process occurs instantaneously. In reality, this is a complex process. As a simplification, the gas is assumed to behave ideally, and the expansion is assumed to be isentropic. The charge, commercially known as PETN, is packed inside a strand made of polyester sheath (Fig. 3a). The PETN ignites at an initial temperature of T_0 (3788 K). It is then assumed to expand isentropically from the packed diameter D_0 to the inner diameter of the polyester sheath D_1 (Fig. 3b). At the end of the expansion, the PETN gas temperature is

$$T_1' = T_0(D_0/D_1)^{2(\gamma-1)} \tag{1}$$

where γ is the specific heat ratio of the PETN gas. Although γ is temperature dependent, a single value was used, based on an average temperature.

The hot PETN gas causes the polyester sheath to gasify at a temperature of 1467°R, and the gasified polyester mixes with the PETN gas. The temperature of mixed gas can be calculated from the energy balance equation. Letting $U(T)$ represent the energy at temperature T, the energy balance equation can be written as

$$U_{12}(T_{12}) = U_1(T_1') + U_2(T_2) - \Delta U(T_a - > T_2) - Q_2 \tag{2}$$

Equation (2) can be written in the following form:

$$(M_1+M_2)C_{12}T_{12} = M_1C_1T_1+M_2C_2T_2-M_2C_2(T_2-T_a)-M_2Hg_2 \tag{3}$$

Solving Eq. (3) for the mixed gas temperature, we find

$$T_{12} = \frac{\{M_1C_1T_1' + M_2[C_2(T_a - Hg_2)]\}}{(M_1 + M_2)C_{12}} \tag{4}$$

The specific heat of the mixed gas C_{12} is calculated by using the mass fraction law:

$$C_{12} = \frac{(M_1C_1 + M_2C_2)}{(M_1 + M_2)} \tag{5}$$

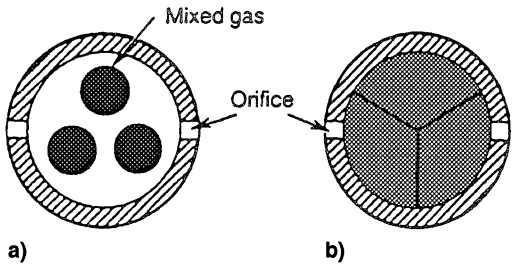

Fig. 4 Gas expansion in an inner tube.

Figure 4a shows an inner tube with the mixed gas generated by three strands of charge, which later expand to the inner diameter of the inner tube, as shown in Fig. 4b. The gas temperature at this stage of expansion is

$$T = T_{12}\left[N(D_2/D_i)^2\right]^{(\gamma-1)} \tag{6}$$

where N is the number of strands in the inner tube and, for this case, $N = 3$.

Recalling the coupled gas/structure model in Fig. 2, the inner tube is represented by subcell A. The density of the mixed gases can be calculated from the density of the PETN gas constituents and the polyester gas constituents. The pressure of the mixed gas can then be calculated by the gas equation:

$$p = R\rho T \tag{7}$$

where R is the universal gas constant.

The gas flow through the orifice into other subcells occurs after this time. The gas flow between adjacent subcells and the mixing of gas in each subcell will be updated in each time step. The numerical bookkeeping of the gas temperature, mass density, and pressure in each subcell will be described in the "Numerical Analysis Procedure" section.

Governing Equations of the Coupled System

The equations of motion of a free–free PLF segment can be written in the following form:

$$[M]\{\ddot{u}\} + [K]\{u\} = \{F(t)\} \tag{8}$$

where the mass and stiffness matrices can be constructed by a finite element program such as NASTRAN. The vector $\{u\}$ represents the physical degrees of freedom (DOFs) defined in the finite element model. The standard eigenvalue solution for Eq. (8) yields the normal mode frequencies $[\omega_n^2]$ and modes $[\phi_n]$. To enhance the interface force resolution at the separation joints, the normal modes are augmented by a set of attachment modes[2] at the location of the rivets. Because the structure is unrestrained, rigid-body modes must be removed; i.e., the inertial-relief procedure must be used prior to the calculation of attachment modes.[2] The attachment modes selected are those associated with the DOFs in the direction of separation forces along the PLF separation joint. The augmented modes are written in the following form:

$$[\phi_n \phi_a] = [\phi] \tag{9}$$

and the coordinate transformation between the physical coordinates and the modal coordinates becomes

$$\{u\} = [\phi]\{q\} \tag{10}$$

Performing a coordinate transformation on Eq. (8), it can be shown that the equations of motion in modal coordinates can be written in the following form[2]:

$$\begin{bmatrix} I & 0 \\ 0 & m \end{bmatrix} \begin{Bmatrix} \ddot{q}_n \\ \ddot{q}_a \end{Bmatrix} + \begin{bmatrix} \omega^2 & 0 \\ 0 & k \end{bmatrix} \begin{Bmatrix} q_n \\ q_a \end{Bmatrix} = [\phi]^T\{F(t)\} \tag{11}$$

where

$$[m] = [\phi_a]^T[M][\phi_a], \qquad [k] = [\phi_a]^T[K][\phi_a]$$

Solving the eigenvalue problem associated with Eq. (11) yields the final frequency and mode shape matrices $[\Omega^2]$ and $[\Phi]$ with the following coordinate transformation:

$$\begin{Bmatrix} q_n \\ q_a \end{Bmatrix} = [\Phi]\{Q\} \tag{12}$$

Applying the coordinate transformation on Eq. (11) and adding modal damping, the equations of motion become

$$\{\ddot{Q}\} + [2\zeta\Omega]\{\dot{Q}\} + [\Omega^2]\{Q\} = [\Phi]^T[\phi]^T\{F(t)\} \tag{13}$$

The applied forces $F(t)$ in Eq. (13) consist of two parts: the bellows separation forces and the rivet resistance forces. They are all functions of relative motion between the two adjacent rails at the separation joints. By using the coordinate transformations

$$\{u\} = [\phi]^T[\Phi]^T\{Q\} \tag{14}$$

these forces can be expressed as functions of the generalized displacements $\{Q\}$. Therefore, the governing equations in Eq. (13) for the coupled gas/structural model are a decoupled set of equations of motion with nonlinear applied forces:

$$\{\ddot{Q}\} + [2\zeta\omega]\{\dot{Q}\} + [\omega^2]\{Q\} = [\Phi]^T[\phi]^T(\{F_p(Q)\} + \{F_r(Q)\}) \tag{15}$$

Equation (15) can be solved numerically. Note that the terms on the left-hand side are a set of uncoupled equations and, therefore, the convolution integral solution[3] can be used in the numerical integration process. However, the nonlinear forces on the right-hand side present some difficulty. To overcome the difficulty, two approximation methods are commonly used as follows: 1) use a very small integration time step and calculate the forces by using displacements from the previous time step, or 2) use the normal integration time step, but perform iteration on the applied forces by using new calculated displacements until the forces converge. The first approach was adopted for the numerical simulation used in the fairing separation analysis. An integration time step of 2 μs was used, and the analytical results compare well with the full-scale test data. The detailed numerical procedure is described in the next section.

Numerical Solution Procedure

The first step of solving Eq. (13) is to calculate the applied forces on the right-hand side of the equation. The procedure to calculate the bellows thrust force is explained first.

Recall that the gas model of the coupled system consists of interconnected subcells with orifices between the subcells. At time t_i, the inner tube of a typical cell is filled with mixed gas with known mass density, temperature, and pressure. Starting at the time of detonation, gas flow through an orifice is due to the pressure difference between the two subcells on the two sides of the orifice, with the direction of the gas flow from high to low pressure. Let the subcells of higher pressure and lower pressure be designated as the upstream and downstream sides of the connecting orifice, respectively. The ratio of downstream pressure and upstream pressure determines whether the orifice flow is choked or unchoked. The pressure ratio is defined as

$$p_r = p_d/p_u \tag{16}$$

For unchoked flow, $p_r \geq c_4$, the mass flow rate through the orifice is

$$\dot{w} = A\left[\frac{c_1 c_2 p_u}{T_u^{0.5}}\right] \tag{17}$$

For choked flow, $p_r < c_3$, the mass flow rate can be written as

$$\dot{w} = A\left[\frac{c_4 p_u}{T_u^{0.5}}\right] \tag{18}$$

where γ is the specific heat ratio and

$$c_1 = [2/(R\gamma_1)]^{0.5}, \qquad c_2 = \left(1 - p_r^{\gamma_3}\right)^{0.5} p_r^{\gamma_5}, \qquad c_3 = (2/\gamma_2)^{\gamma_4}$$

$$c_4 = \left[(\gamma/R)(2/\gamma_2)^{\gamma_6}\right]^{0.5}, \qquad \gamma_1 = (\gamma - 1)/\gamma, \qquad \gamma_2 = \gamma + 1$$

$$\gamma_3 = \gamma - 1 \gamma_4 = \gamma/(\gamma - 1), \qquad \gamma_4 = \gamma/(\gamma - 1)$$

$$\gamma_5 = 1/\gamma, \qquad \gamma_6 = (\gamma + 1)(\gamma - 1)$$

Equations (17) and (18) assume loss-free (isentropic) flow through the orifice. Once the mass flow rate through each orifice in the gas model is determined at a given time step, the net mass flow rate into each subcell can be determined by subtracting the outflow rate from the inflow rate, i.e.,

$$\dot{w} = \sum \dot{w}_{\text{in}} - \sum \dot{w}_{\text{out}} \tag{19}$$

The accumulation of gas flow in a typical subcell between the nth time step and the $(n + 1)$th time step can be calculated by the following integration formula:

$$m_{n+1} = m_n + \alpha \dot{w}_n \Delta t + (1 - \alpha)\dot{w}_{n+1} \Delta t \tag{20}$$

where α is the Newmark integration constant[4] and Δt is the integration time step. If the volume of the subcell is known, the mass density ρ in each subcell can be calculated as

$$\rho_{n+1} = m_{n+1}/v_n \tag{21}$$

In Eq. (21), the volume is written in a general form to allow for change as a function of time such as occurs in subcell C, although the volumes in subcells A and B are constant. The volume of subcell C is approximated by the volume at the previous integration time step n.

The gas temperature of the previous time step is modified by the temperature of the incoming and outgoing gas. Because the volumes of subcells A and B remain constant, the updated gas temperature of the subcell is calculated by using the following mixing formula:

$$T_{n+1} = \frac{\left[T_n m_n + \Delta t \sum_{\text{in}} T_n \dot{w}_{n+1} - \Delta t \sum_{\text{out}} T_n \dot{w}_{n+1}\right]}{m_{n+1}} \tag{22}$$

To calculate the gas temperature in the expanding bellows (subcell C), the isentropic expansion formula is used:

$$T_{n+1} = \frac{\left[T_n m_n + \Delta t \sum_{\text{in}} T_n \dot{w}_{n+1} - \Delta t \sum_{\text{out}} T_n \dot{w}_{n+1}\right]}{\left[m_{n+1} v_r^{\gamma - 1}\right]} \tag{23}$$

where $v_r = v_n(Q_{n-1})/v_{n+1}(Q_n)$, which depends on local displacement.

The updated pressure in each subcell becomes

$$p_{n+1} = R\rho_{n+1} T_{n+1} \tag{24}$$

The rivet-resistant forces are also a function of displacement. The force-displacement relationship can be obtained from rivet shear test data.

The fairing deformation in a dynamic analysis is usually defined at the nodal points of the finite element model along the separation joint. The locations of the gas cell or the rivet seldom coincide with the nodal point. To provide a smooth interpolation of the displacement at each individual rivet or gas cell, a cubic spline curve-fitting[5] procedure was used, and the rivet-resistant forces and the bellows thrust forces were calculated, based on this local displacement. They were then lumped back to the nodal points to form the bellows and rivet forces in Eq. (13).

Comparison of Results with Test Data

The fairing model used in the fairing separation analysis was a 60-deg, half-trisector finite element model. The following assumptions were made to justify the use of a half-model: each fairing trisector deforms symmetrically with respect to its spine, and all three trisectors have identical responses. A total of 322 modes (normal plus attachment modes) of the fairing model were retained, with a cutoff frequency of 250 Hz for the normal modes. The number of attachment modes was equal to the number of nodes along the separation joint. The gasdynamics model in the separation joint consisted of 200 gas cells. This coupled gasdynamic model was used to simulate the separation dynamic events of the two full-scale AEDC separation tests.

The instrumentation plan of the AEDC full-scale tests included the following: pressure transducers located at 0, 52, 437, and 653 in. from the bottom of the fairing to measure the pressure transients inside the bellows and high-speed cameras to measure the c.g. velocity and pitch rate of the separating PLF trisectors.

The digitized records of pressure transients for the three separation joints were plotted on top of the analytical results as shown in Figs. 5 and 6 for the flight and force-margin test configurations, respectively. As can be seen, the agreement is excellent. Because the three PLF trisectors used in the test article resemble each other in weight and stiffness, the measured separation velocities and pitch rates were very close. Therefore, the average values were used for comparison with the analytical results, as shown in Table 1. Again,

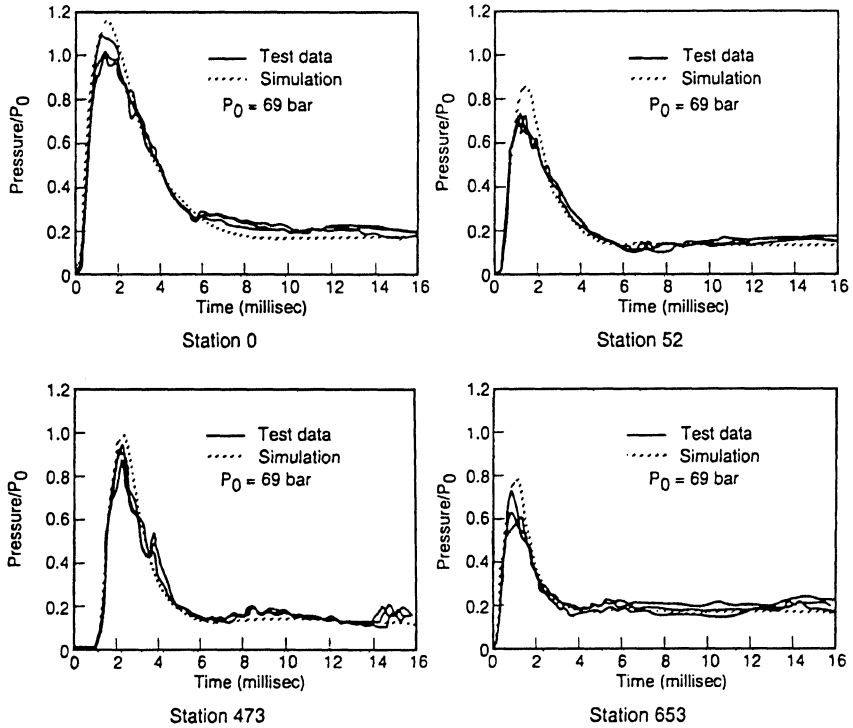

Fig. 5 Comparison of bellows pressure transients for flight configuration.

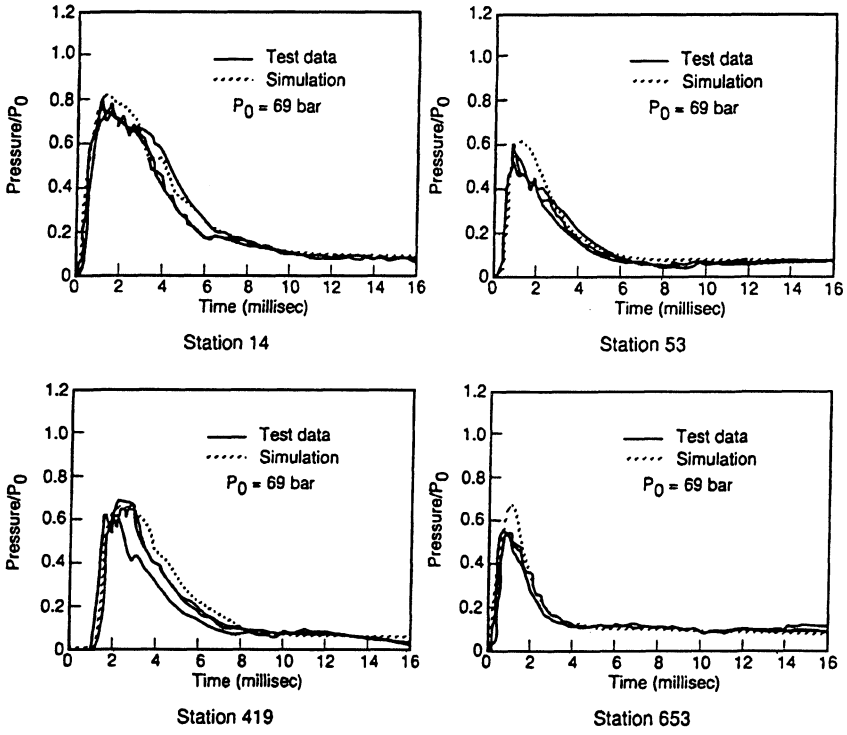

Fig. 6 Comparison of bellows pressure transients for force margin test configuration.

Table 1 Comparison of fairing separation rates

	Three-strand case		Two-strand case	
Rate	Test data	Prediction	Test data	Prediction
C.G. velocity, m/s	5.64	5.49	4.21	4.12
Pitch rate, deg/s	19.00	18.30	15.00	15.05

the comparison between the test data and the analytical results shows good agreement.

Conclusion

An analytical procedure has been developed to simulate the PLF separation dynamics, based on a coupled gas/structure model. The validity of the analysis procedure has been verified by full-scale test data. Successful correlation with the test data is attributed to two ingredients in the formulation of the analysis procedure: 1) sufficient detail in the gas model to describe the expansion of PETN gas and subsequent gas flow in the attenuation tubes and bellows and 2) the use of attachment modes in the PLF model to enhance the calculation of interface forces at the separation joint.

The fleet of Titan IV vehicles has PLFs of different lengths with the same separation joint designed to accommodate different payload sizes. It is not practical to verify all of them by test. Last-minute design changes in the fairing separation system are also quite common. The analytical procedure developed here provides an inexpensive tool to assess the flightworthiness of those PLFs that are not test verified.

Acknowledgments

This work was performed from July 1986 to June 1990 as a part of The Aerospace Corporation's general system engineering and integration support to the Titan Program Office. During the course of the development and validation of the analytical procedure and the computing code, numerous informal communication and data exchanges took place between personnel from The Aerospace Corporation, Lockheed Martin, and McDonnell Douglas Astronautics. In particular, extensive discussions were held with J. Williams of Lockheed Martin and C. A. Van Ornum of McDonnell Douglas Astronautics. Their cooperation, contributions, and courtesy are greatly appreciated. The author would also like to thank Alvar M. Kabe, Erwin Perl, and Robert G. Wagner of The Aerospace Corporation for their encouragement and guidance for this work.

References

[1]Cheng, S.-C., "Payload Fairing Analysis," The Aerospace Corporation, Aerospace TM 89(4530-02)-20, Los Angeles, CA, April 1989.

[2]Chang, C.-J., "A General Procedure for Substructure Coupling in Dynamics Analysis," Ph.D. Dissertation, Engineering Mechanics Dept., Univ. of Texas, Austin, TX, Dec. 1977.

[3]MacNeal, R. (ed.), *The NASTRAN Theoretical Manual*, NASA SP-221(01), Dec. 1972.

[4]Newmark, N. M., "A Method for Computation for Structural Dynamics," *ASCE Journal of Engineering Mechanics Division*, Vol. 85, July 1959, pp. 67–94.

[5]Forsythe, G. E., Malcolm, M. A., and Moler, C. B., *Computer Methods for Mathematical Computations*, Prentice–Hall, Englewood Cliffs, NJ, 1977, pp. 89–91.

F. H. Lutze Jr.
Associate Editor